

Quantum Image Fusion Methods for Remote Sensing

Leslie Miller
SenSIP Center, School of ECEE
Tempe, AZ 85287
lmille42@asu.edu

Glen Uehara
SenSIP Center, School of ECEE
Tempe, AZ 85287
guehara@asu.edu

Andreas Spanias
SenSIP Center, School of ECEE
Tempe, AZ 85287
spanias@asu.edu

Abstract—This paper presents algorithms, simulations, and results using machine learning and quantum image fusion algorithms for radar and remote sensing applications. Previous efforts in the classification of synthetic aperture radar (SAR) images using quantum machine learning provided encouraging results but, nevertheless modest accuracy. In this paper, we propose a novel quantum image fusion technique used for identifying and classifying objects obtained from C-band SAR and optical images. More specifically, we design a four-qubit quantum circuit to process the SAR image dataset. This method enhances the spectral details otherwise not seen when using the raw SAR dataset. In addition to the quantum circuit, we design deep neural networks (NN) to improve classification results. The Visual Geometry Group 16 (VGG16), a convolutional neural network that is sixteen layers deep, is customized and used for classification. The merit of quantum fusion as well as the promising results in improving the overall system and the potential of lowering size, weight, power, and cost (SWaP-C) is described.

TABLE OF CONTENTS

1. INTRODUCTION.....	1
2. CLASSICAL IMAGE FUSION	2
3. QUANTUM IMAGE FUSION	3
4. DISCUSSION OF RESULTS.....	5
5. CONCLUSION	7
ACKNOWLEDGEMENTS	7
REFERENCES	7
BIOGRAPHY	9

1. INTRODUCTION

Image fusion is a powerful image processing tool that has received significant attention in the field of remote sensing and image processing since the mid-nineteen eighties [1]. Image fusion enhances our ability to extract meaningful information and can be deployed in various applications, including medical imaging, aerospace applications, remote sensing, military surveillance, and manufacturing flaw identification [2,3,4].

Related Work

More recently, quantum image fusion studies have been reported along with their feasibility and applications in [5,6,7]. In [5], quantum fusion for optical and SAR image datasets was presented. The authors used eight different

quantum fusion techniques to process and fuse their dataset, which consisted of 1900 images.

They used a deep learning model, realized by convolutional neural networks, to train the binary set of fused images. In [6] quantum wavelet transforms and sum-modified-Laplacian rules were used for image fusion. This technique found applications in medical image fusion and using visible and infrared images to perform fusion. Paper [7] shows applications of quantum image processing for CT and MRI fusion.

Previous Work

In our previous SAR classification efforts [8] we used quantum machine learning (QML) for image classification tasks. More specifically, our previous work focused on developing a hybrid Quantum-classical model that was trained on SAR images. Classical computing classification using neural networks produced a training accuracy of 77.19%, while our hybrid quantum classification neural network architecture resulted in produced 64.14% accuracy [8]. The relatively low accuracy was attributed to the limited training of the QCNN algorithm due to restricted computing resources.

Current Work and Contributions

Our study, reported in this paper, addresses image classification using enhanced feature extraction, fusion, and the use of single qubit operations where GPU-based quantum simulations can provide improved speed. By using a quantum circuit to process the SAR dataset and using fusion techniques to combine the optical images with the quantum processed SAR dataset, we extract more robust features. The quantum fused dataset is used to train a deep learning algorithm, more specifically, the Visual Geometry Group 16 (VGG16) [8, 9] architecture. This approach improved classification results relative to our previous study [8].

Our contributions to this study are: a) improving the quantum circuit used for quantum image fusion, b) showing the reduction in computational complexity using our proposed quantum method, and c) demonstrating a reduction in SWaP-C. We note that our work is different than [5] in that: we a) add unitary gates to our quantum circuit, b) train on a different and larger dataset of images, c) use a different deep learning model, and d) perform multi-class scene classification.

The image data used in this study comes from the SEN1-2 dataset. The dataset consists of 282,384 pairs of image patches. The images were collected across the globe and include various meteorological seasons [10]. Figure 1 shows the paired optical and SAR images for each of the four classes.

Applications and Challenges

Although this work has several applications, we highlight specifically some of the important applications in the aerospace industry. By combining the same scene images from multisource imagery, we get an enhanced image with

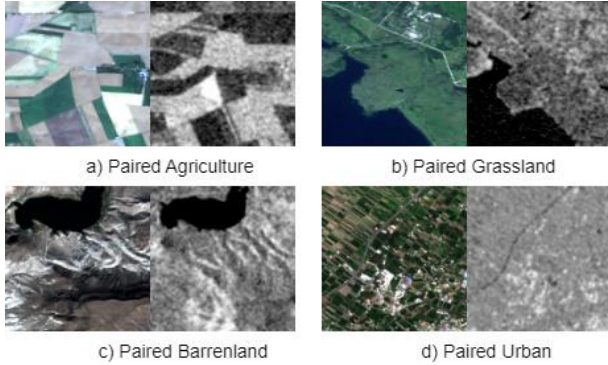


Figure 1. Paired SAR and Optical Images from various scenes: agriculture, grassland, barrenland, and urban.

completeness of spectral information [11]. Fusion can be used to enhance certain features not seen in either single dataset alone, sharpen images, improve reliability, and improve classification [12]. Quantum image processing techniques have the potential to extract important details and features faster and more accurately. This could be useful in object identification and tracking applications [11], image segmentation [11], land mapping [13], and regional change detection [11]. Quantum image fusion also has the potential to lower the size, weight, power, and cost of the system (SWaP-C) [13,14].

Some of the challenges we faced in our studies are long processing times when using quantum fusion techniques, limited access to quantum hardware resulting in the use of Qiskit simulators, and a small number of qubits. It is expected that as progress is made in quantum computing and hardware access becomes easier, we will be able to demonstrate a quantum advantage in computation processing time.

This paper is organized as follows, Section 2 describes the classical ML model, Section 3 presents the quantum fusion design process, Section 4 is our discussion of results, and Section 5 presents our conclusions.

2. CLASSICAL IMAGE FUSION

We began this research by exploring two methods for classical image fusion. A VGG16 [8] convolutional neural network is used to train and classify the classically fused dataset. The results from classical fusion serve as a baseline to compare our quantum fusion model to.

Classical Fusion with Machine Learning

We use two methods to perform classical image fusion, which are described below. We divide and process the optical image dataset in terms of three channels, namely, red, green, and blue for both methods.

Method I

The first classical fusion method used was the Brovey Transform (BT) [16]. The BT multiplies each multispectral band with the SAR image. Each product is then divided by the total sum of the multispectral bands. The three new channels are then stacked. The mathematical representation is shown in equations 1,2,3, and 4, where R=red channel, B=blue channel, G=green channel, S=SAR, and MF = Mathematical Fusion.

$$\text{Red}_{\text{new}} = \left(\frac{R}{(R+G+B)} \right) \times S \quad (1)$$

$$\text{Blue}_{\text{new}} = \left(\frac{B}{(R+G+B)} \right) \times S \quad (2)$$

$$\text{Green}_{\text{new}} = \left(\frac{G}{(R+G+B)} \right) \times S \quad (3)$$

$$\text{MF} = \text{stack}(\text{Red}_{\text{new}}, \text{Blue}_{\text{new}}, \text{Green}_{\text{new}}) \quad (4)$$

Method II

The second classical fusion method used is described by equations 5,6, and 7 [5].

$$\text{Red}_{\text{new}} = \left(\frac{S+3 \times R}{4} \right) \quad (5)$$

$$\text{Blue}_{\text{new}} = \left(\frac{S+3 \times B}{4} \right) \quad (6)$$

$$\text{Green}_{\text{new}} = \left(\frac{S+3 \times G}{4} \right) \quad (7)$$

The new red, green, and blue channels were then stacked. To perform image classification, each fusion method was processed using a VGG16 architecture.

Due to longer processing times, we use a subset of the original dataset. This subset contains 4,000 quantum fused images. To provide a more comprehensive assessment of our model, we performed the experiment four times, each time using a different subset of images. We then average the results. Due to an outlier in the results for the four subsets of images, we note we limited our averaging analysis to three subsets. The presence of an outlier can be attributed to extreme brightness, due to a portion of the dataset coming from the summer season. The outlier can be corrected

through normalization techniques and will be a central focus in our future research.

A brief discussion of our results are as follows. The best performing simulation for the classical fusion was Method I, achieving a validation accuracy of 93.16% and a training accuracy of 94.73%. When averaging, Method I maintained the highest validation and training accuracy compared to the classical fusion Method II with an average validation accuracy of 83.84% and average training accuracy of 93.09%. Section

3. QUANTUM IMAGE FUSION

Quantum Fusion Method

The overall architecture of our quantum fusion model can be seen in, Figure 2 which shows the separation of the optical image into three channels, the denoising filter, the quantum circuit, and the fusion stage.

We first separated each of our four classes of data, namely, agriculture, barrenland, grassland, and urban, and we formed two subsets, namely SAR and optical. SAR images have

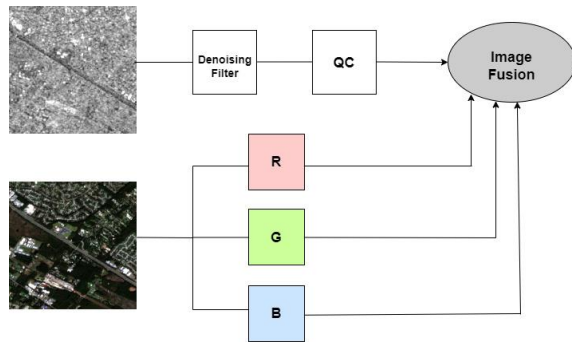


Figure 2. Quantum Fusion Architecture with Denoising Filter, Quantum Circuit, and Split Optical Channels.

speckle effects and are generally complex to process. To denoise the SAR dataset, a Lee Filter was used [17]. The Lee filter was chosen because it was previously used successfully for despeckling and noise removal in the radar image processing field [18].

We then separate the optical image into three channels: red, green, and blue. Then, we process the SAR image with a 4-qubit quantum circuit. Details of the quantum circuit can be seen in Section 3, Quantum Circuit and Feature Extraction. Once the SAR channel is processed through the quantum circuit, the optical channels are combined with the quantum processed SAR channel using a fusion method. To process the raw quantum features, we use two different fusion processes. We use Method II, which is described in equations 5,6 and 7, where S is the quantum processed SAR channel. The other fusion method used is described below in *Method III*.

Method III

Method III uses averaging to perform image fusion [5]. Equation 8 describes Method III where R=red, B=blue, G=green, and S= Quantum Processed SAR.

$$\left(\frac{S+R+G+B}{4}\right) \quad (8)$$

Once the quantum fusion process is completed, the original 256x256 image is transformed to a 64x64 quantum processed image. We then use deep learning to classify our dataset. The VGG16 neural network is discussed further in Section 3.

Quantum Circuit and Feature Extraction

We utilized IBM's Qiskit to program and simulate the quantum circuits [19, 20]. To perform quantum fusion, we used a 4-qubit quantum circuit that was two layers deep. This circuit can be seen in Figure 3. To perform feature extraction, we include in our circuit Ry gates, unitary gates, and the Pauli-X, Pauli-Y, Pauli-Z, and Hadamard gates [8, 21, 22]. The Ry gates perform single-qubit rotations around the y-axis. We include 4 Ry gates before the unitary gates. Details about the Pauli-X, Pauli-Y, Pauli-Z, Hadamard, and Ry gates can be found in Table 1.

The unitary gates are a set of gates that perform rotations through weights that change continuously [8, 21]. We note that in this research, we wanted to move from an entangled

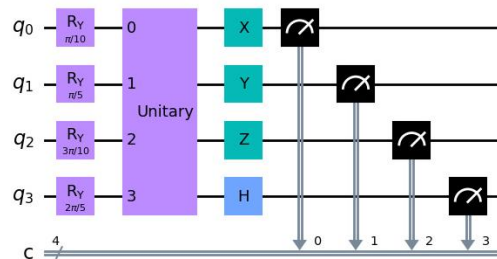


Figure 3. Four Qubit Quantum Circuit (QC) for the Processing of SAR Images.

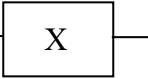

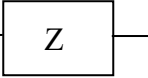
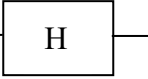
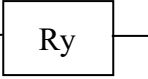
circuit previously researched in [8] to another method using unitary random gates. The unitary is added to either twirl, distribute, or help with gate fidelity. This method is based on the Haar measure [23]. We initially ran randomized gates on each of the qubits to identify which random set of gates worked best for our problem. Once the best set of gates is established, the unitary model is saved and used for image fusion. After the Ry rotations and unitary gates, we used a Pauli-X, Pauli-Y, Pauli-Z, and Hadamard gate. The Pauli-X gate performs a single-qubit rotation around the x-axis, the Pauli-Y gate performs a single-qubit rotation around the y-axis, the Pauli-Z gate performs a single-qubit rotation around



Figure 5. VGG16 with 13 Convolutional Layers and 3 Fully Connected Layers [8].

the z axis, and the Hadamard gate performs rotations about the $(\hat{x} + \hat{z})/\sqrt{2}$ axis [24,25].

Table 1. Quantum gates used in our studies.

Gate	Representation	Matrix
Pauli-X		$\begin{pmatrix} 0 & 1 \\ 1 & 0 \end{pmatrix}$
Pauli-Y		$\begin{pmatrix} 0 & -i \\ i & 0 \end{pmatrix}$
Pauli-Z		$\begin{pmatrix} 1 & 0 \\ 0 & 1 \end{pmatrix}$
Hadamard		$\frac{1}{\sqrt{2}} \begin{pmatrix} 1 & 1 \\ 1 & -1 \end{pmatrix}$
Ry Gate		$\begin{pmatrix} \cos(\frac{\theta}{2}) & -\sin(\frac{\theta}{2}) \\ \sin(\frac{\theta}{2}) & \cos(\frac{\theta}{2}) \end{pmatrix}$

After the quantum fusion operations, a 64x64 pixel image is produced. This is then processed using the VGG16 neural network architecture. Figure 4 shows an example of the before and after of our newly processed quantum image for one of the classes of images.

Neural Network Model

We describe here the use of QML for SAR image classification. We note that the merit and tradeoffs of ML and QML have also been studied before for various applications including audio and image classification, and photovoltaic fault detection [24,26,27,29]. For this particular imaging study, we describe algorithmic steps as follows.

After we have carefully preprocessed our images, we use a classical neural network architecture to perform the scene classification task. In this paper, we use the VGG16 algorithm to perform scene classification. We chose to use the VGG16 because it has previously been used successfully in image and vision recognition tasks [29]. The VGG16 consists of 16 layers with trainable weights, effectively mitigating the need for a large number of hyper-parameters [30]. The VGG16 architecture can be seen in Figure 5.

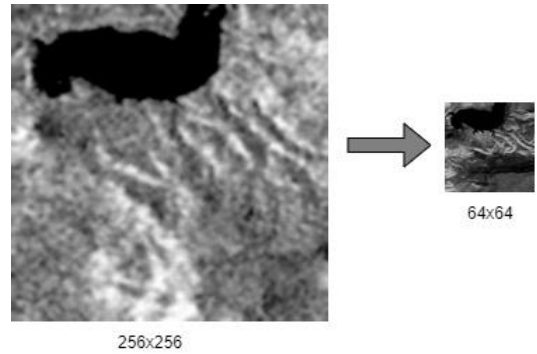


Figure 4. 256x256 SAR Image to 64x64 Quantum Processed SAR Image, Quantum Fusion Method III.

The Keras machine learning package is used to implement the quantum circuit and perform machine learning [20]. The Adam optimizer is used to adjust the parameters of the VGG16 in real-time. This helps improve the speed and accuracy of the algorithm [30]. Figure 6 shows the overall implementation of our model with quantum fusion.

In the case of Quantum Method II, the best-performing simulation achieved a training accuracy of 92.77% and a validation accuracy of 84.04%. For Quantum Method III, the best-performing simulation resulted in a training accuracy of 96.03% and validation accuracy of 93.75%. Using image fusion and the VGG16 architecture, we achieved an averaged validation accuracy of 86.79% for the Quantum Method III and an average validation accuracy of 75.42% for Quantum Method II. Detailed results are presented in Section 4.

Advantages and Challenges

There were a few challenges encountered when performing quantum fusion. We experienced longer runtimes than the classical model when performing the fusion. We were also limited on the number of qubits we could use. We used the Qiskit simulator to simulate the quantum circuit used for the processing of the SAR dataset. To simulate operating on real quantum hardware and simulate the potential noise effects,

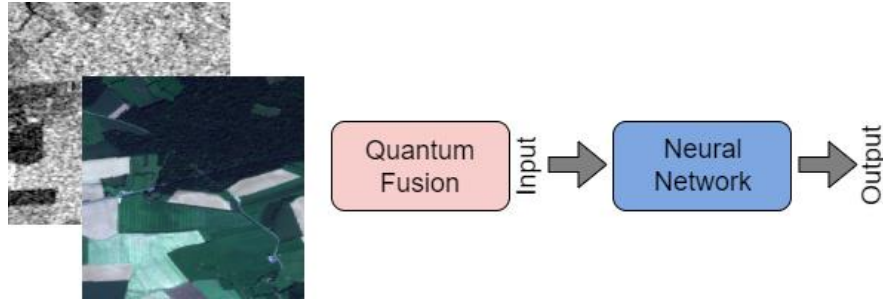


Figure 6. Implementation of our model with Quantum Fusion.

we used IBM’s Fake Vigo [31]. This is a quantum simulator provided by Qiskit for simulating the behavior of the IBM Q Vigo quantum device. There was a ~2% decrease in classification accuracy when simulating the IBM Q Vigo quantum hardware with quantum noise [31,32]. In the next step, we will look at the fidelity distribution, and purity of the unitary matrix to minimize the fundamental gates for quantum hardware compatibility. We will also explore using more advanced IBM quantum hardware simulators.

There are several advantages realized with quantum fusion and they are:

- Reduction in Computational Complexity
- Reduction in Memory
- Higher Classification Accuracy
- Use of lower resolution images

Overall, we note that quantum fusion led to a reduction in computational complexity relative to our previous quantum model [8]. Quantum fusion also led to a reduction in memory requirements, higher accuracy, and higher classification accuracy for lower resolution images. The complexity of the quantum fusion algorithm is described in Equation 9. The runtime computational complexity of this algorithm is of order N and hence, it has a linear relationship with the number of qubits used [33,34].

$$O(N), \text{ where } N = \text{number of qubits} \quad (9)$$

The quantum fusion Method III gave us almost 30% higher accuracy from our previous quantum model and outperformed both classical fusion methods [8]. The algorithm demonstrates the ability to achieve high classification accuracy with smaller 64x64 images. In addition to a reduction in complexity and higher classification accuracy, the quantum fusion method resulted in a 75% reduction in memory compared to the classical fusion method. The reduction in memory coupled with the reduced complexity offers several advantages. Furthermore, as quantum technology advances, there is promise in the optimization and reduction of SWaP-C. Quantum fusion has

the potential to provide better system performance, lower power consumption, and be cost effective.

4. DISCUSSION OF RESULTS

We performed classical and quantum fusion and ran our dataset through a classical VGG16 algorithm. Quantum Fusion Method III performed the best with an average validation classification accuracy of 86.79%. The second best was the classical fusion Method I with an average validation classification accuracy of 83.84%.

The results reported in Table 2 and Table 3 presents the outcomes of three separate model training runs, conducted on different subsets of the dataset. Table 4 shows the final averaged values for the classical and quantum methods, providing a comprehensive assessment of the overall performance.

Table 2. Classical Fusion Results.

Method	Data size (train vs validation)	Accuracy (train vs validation)
Method I	Train: 3200 Validation: 800	Train: 94.73 Validation: 93.16
Method I	Train: 3200 Validation: 800	Train: 93.53 Validation: 85.14
Method I	Train: 3200 Validation: 800	Train: 91 Validation: 73.23
Method II	Train: 3200 Validation: 800	Train: 84.28 Validation: 72.3
Method II	Train: 3200 Validation: 800	Train: 83.89 Validation: 62.25
Method II	Train: 3200 Validation: 800	Train: 88.48 Validation: 71.79

Table 3. Quantum Fusion Results.

Method	Data size (train vs validation)	Accuracy (train vs validation)
Method II	Train: 3200 Validation: 800	Train: 88.51 Validation: 81.12
Method II	Train: 3200 Validation: 800	Train: 85.56 Validation: 61.06
Method II	Train: 3200 Validation: 800	Train: 92.77 Validation: 84.04
Method III	Train: 3200 Validation: 800	Train: 94.83 Validation: 89.1
Method III	Train: 3200 Validation: 800	Train: 93.06 Validation: 77.53
Method III	Train: 3200 Validation: 800	Train: 96.03 Validation: 93.75

Table 4. Averaged Classical and Quantum Results.

Method	Data size (train vs validation)	Accuracy (train vs validation)
Classical Fusion Method I	Train: 3200 Validation: 800	Train: 93.09 Validation: 83.84
Classical Fusion Method II	Train: 3200 Validation: 800	Train: 85.55 Validation: 68.78
Quantum Fusion Method II	Train: 3200 Validation: 800	Train: 88.96 Validation: 75.42
Quantum Fusion Method III	Train: 3200 Validation: 800	Train: 94.64 Validation: 86.79

Figure 7 and Figure 8 show the training loss and accuracy curves for the averaged classical fusion and averaged quantum fusion methods. Figure 9 and Figure 10 show the validation loss and accuracy curves for the averaged fusion methods.

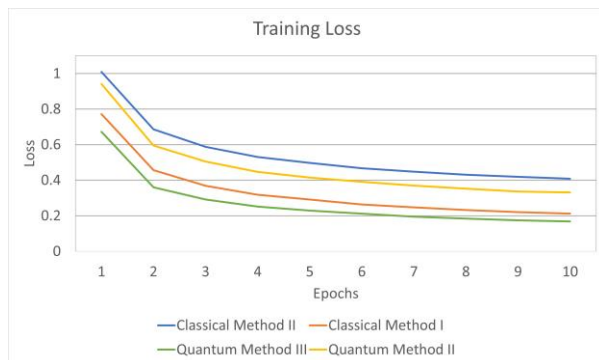


Figure 7. VGG16 Training Loss Curve for the two classical and two quantum methods described.

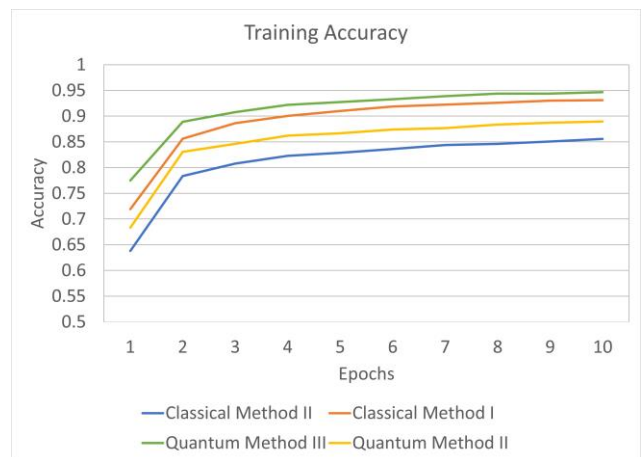


Figure 8. VGG16 Training Accuracy Curve for the two classical and two quantum methods described.

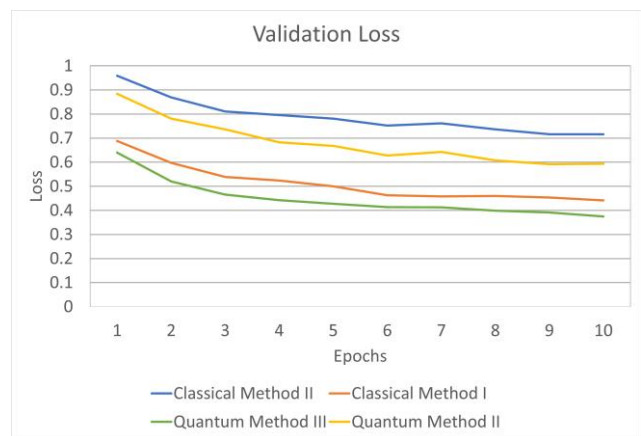


Figure 9. VGG16 Validation Loss Curve for the two classical and two quantum methods described.

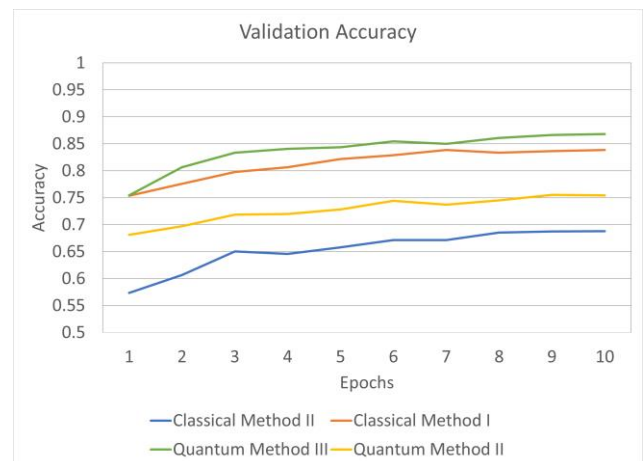


Figure 10. VGG16 Validation Accuracy Curve for the two classical and two quantum methods described.

5. CONCLUSION

In this work, we proposed a novel way to use quantum circuits to process the SAR dataset and perform image fusion and classification. We compared the accuracy of the quantum image fusion to classical image fusion. We found that the overall quantum fusion system led to a reduction in memory and has the future potential to lower the SWaP-C metric.

We observed that smaller image sizes can still result in a high accuracy, and the quantum circuit we proposed led to a reduction in complexity. Future work includes optimizing the current quantum fusion algorithm, train for longer and utilize the full dataset, and incorporate quantum value calculations into our model [35]. In addition to the above, we look to incorporate quantum error mitigation and executing our model on quantum hardware.

6. ACKNOWLEDGEMENTS

Support for this project was provided by the Quantum Collaborative, the SenSIP center, and an NSF REU supplement.

REFERENCES

- [1] Y. Zhang, "Understanding Image Fusion," *Photogrammetric Engineering and Remote Sensing*, vol. 70, pp. 657-661, 2004.
- [2] Wei, Lin, Haowen Liu, Jing Xu, Lei Shi, Zheng Shan, Bo Zhao, and Yufei Gao. "Quantum machine learning in medical image analysis: A survey." *Neurocomputing* 525 (2023): 42-53.
- [3] Senokosov, A., Sedykh, A., Sagingalieva, A. and Melnikov, A., 2023. Quantum machine learning for image classification. arXiv preprint arXiv:2304.09224.
- [4] Z. Omar and T. Stathaki, "Image Fusion: An Overview," 2014 5th International Conference on Intelligent Systems, Modelling and Simulation, Langkawi, Malaysia, 2014, pp. 306-310.
- [5] Majji, Sathwik Reddy, Avinash Chalumuri, Raghavendra Kune, and B. S. Manoj. "Quantum processing in fusion of SAR and optical images for deep learning: A data-centric approach." *IEEE Access* 10 (2022): 73743-73757.
- [6] X. Liu and D. Xiao, "Multimodality Image Fusion Based on Quantum Wavelet Transform and Sum-Modified-Laplacian Rule," *Int J Theor Phys*, vol. 58, pp. 734-744, 2019. [Online].
- [7] R. Shen, I. Cheng and A. Basu, "Cross-Scale Coefficient Selection for Volumetric Medical Image Fusion," *IEEE Transactions on Biomedical Engineering*, vol. 60, no. 4, pp. 1069-1079, April 2013.
- [8] L. Miller, G. Uehara, A. Sharma and A. Spanias, "Quantum Machine Learning for Optical and SAR Classification," 2023 24th International Conference on Digital Signal Processing (DSP), Rhodes (Rodos), Greece, 2023, pp. 1-5.
- [9] G. Learning, "Everything you need to know about VGG16," *Medium*, 23-Sep-2021. [Online]. Available: <https://medium.com/@mygreatlearning/everything-you-need-to-know-about-vgg16-7315defb5918>. [Accessed: 12-Sept-2023].
- [10] M. Schmitt, L. H. Hughes, and X. X. Zhu, "The SEN1-2 dataset for deep learning in SAR-optical data fusion," *ISPRS Annals of the Photogrammetry, Remote Sensing and Spatial Information Sciences*, vol. IV-1, pp. 141-146, 2018.
- [11] Y. Byun, J. Choi and Y. Han, "An Area-Based Image Fusion Scheme for the Integration of SAR and Optical Satellite Imagery," *IEEE Journal of Selected Topics in Applied Earth Observations and Remote Sensing*, vol. 6, no. 5, pp. 2212-2220, Oct. 2013.
- [12] C. Pohl and J. L. Genderen, "Multisensor image fusion in remote sensing: concepts method and applications", *Int. J. Remote Sens.*, vol. 19, no. 5, pp. 823-854, Mar. 1998.
- [13] W. A. Lies, L. Narula, P. A. Iannucci and T. E. Humphreys, "Low SWaP-C Radar for Urban Air Mobility," 2020 IEEE/ION Position, Location and Navigation Symposium (PLANS), Portland, OR, USA, 2020, pp. 74-80.
- [14] "What is swap-C?," BAE Systems | United States, <https://www.baesystems.com/en-us/definition/what-is-swap-c> [Accessed: 19-Sept-2023].
- [15] F. Pacifici, F. Del Frate, W. J. Emery, P. Gamba and J. Chanussot, "Urban Mapping Using Coarse SAR and Optical Data: Outcome of the 2007 GRSS Data Fusion Contest," *IEEE Geoscience and Remote Sensing Letters*, vol. 5, no. 3, pp. 331-335, July 2008.
- [16] I. Misra, R. K. Gambhir, S. M. Moorthi, D. Dhar and R. Ramakrishnan, "An efficient algorithm for automatic fusion of RISAT-1 SAR data and Resourcesat-2 optical images," 2012 4th International Conference on Intelligent Human Computer Interaction (IHCI), Kharagpur, India, 2012, pp. 1-6.
- [17] J.-S. Lee, J.-H. Wen, T. L. Ainsworth, K.-S. Chen and A. J. Chen, "Improved sigma filter for speckle filtering of SAR imagery", *IEEE Trans. Geosci. Remote Sens.*, vol. 47, no. 1, pp. 202-213, Jan. 2009.
- [18] O. Rubel, V. Lukin, A. Rubel, and K. Egiazarian, "Selection of Lee Filter Window Size Based on Despeckling Efficiency Prediction for Sentinel SAR

- Images," Remote Sensing, vol. 13, no. 10, p. 1887, May 2021.
- [19] P. Foy, ["Introduction to quantum programming with Qiskit," MLQ.ai, 12-Dec-2022. [Online]. Available: <https://www.mlq.ai/quantum-programming-with-qiskit/>. [Accessed: 15-Aug-2023].
- [20] "Simple. flexible. powerful.," Keras. [Online]. Available: <https://keras.io/>. [Accessed: 15-Aug-2023].
- [21] M. Esposito, G. Uehara and A. Spanias, "Quantum Machine Learning for Audio Classification with Applications to Healthcare," 2022 13th International Conference on Information, Intelligence, Systems & Applications (IISA), Corfu, Greece, 2022, pp. 1-4.
- [22] D. Voorhoeve, "Ry gate," Quantum Inspire, <https://www.quantum-inspire.com/kbase/ry-gate/> [Accessed: 12-Sept-2023].
- [23] A. A. Mele, "Introduction to Haar Measure Tools in Quantum Information: A Beginner's Tutorial," arXiv preprint arXiv:2307.08956, 2023.
- [24] G. S. Uehara, A. Spanias and W. Clark, "Quantum Information Processing Algorithms with Emphasis on Machine Learning," 2021 12th International Conference on Information, Intelligence, Systems & Applications (IISA), Chania Crete, Greece, 2021, pp. 1-11.
- [25] University of Maryland Ion Trap Group, "Quantum Gates," University of Maryland Ion Trap Group, [Online]. Available: <https://iontrap.umd.edu/wp-content/uploads/2016/01/Quantum-Gates-c2.pdf>. [Accessed: 28-Aug-2023].
- [26] M. Esposito, G. Uehara and A. Spanias, "Quantum Machine Learning for Audio Classification with Applications to Healthcare," 2022 13th International Conference on Information, Intelligence, Systems & Applications (IISA), Corfu, Greece, 2022, pp. 1-4.
- [27] G. Uehara, S. Rao, M. Dobson, C. Tepedelenlioglu and A. Spanias, "Quantum Neural Network Parameter Estimation for Photovoltaic Fault Detection," 2021 12th International Conference on Information, Intelligence, Systems & Applications (IISA), Chania Crete, Greece, 2021, pp. 1-7.
- [28] P. Gohel, A. Chakraborty and K. R. JV, "Organ classification Using Quantum Convolution Network," 2022 IEEE International Conference on Quantum Computing and Engineering (QCE), Broomfield, CO, USA, 2022, pp. 831-832.
- [29] "Beginner's Guide to VGG16 implementation in Keras," Built In, <https://builtin.com/machine-learning/vgg16> [Accessed: 12-Sept-2023].
- [30] S. Mahendra, "What is the adam optimizer and how is it used in machine learning," Artificial Intelligence +, <https://www.aiplusinfo.com/blog/what-is-the-adam-optimizer-and-how-is-it-used-in-machine-learning/#:~:text=The%20Adam%20optimizer%20is%20a%20popular%20algorithm%20used%20in%20deep,its%20historical%20gradients%20and%20momentum> [Accessed: 3-Oct-2023].
- [31] "Fakevigo," IBM Quantum Documentation, https://docs.quantum-computing.ibm.com/api/qiskit/qiskit.providers.fake_provider.FakeVigo [Accessed: 12-Sept-2023].
- [32] T. Patel, A. Potharaju, B. Li, R. B. Roy and D. Tiwari, "Experimental Evaluation of NISQ Quantum Computers: Error Measurement, Characterization, and Implications," SC20: International Conference for High Performance Computing, Networking, Storage and Analysis, Atlanta, GA, USA, 2020, pp. 1-15, doi: 10.1109/SC41405.2020.00050.
- [33] D. Musk, A Comparison of Quantum and Traditional Fourier Transform Computations, https://d197for5662m48.cloudfront.net/documents/publicationstatus/53281/preprint_pdf/b34ed0bc05160ab903a3790ad0dbe450.pdf [Accessed: 15-Sept-2023].
- [34] A. Sharma, G. Uehara, V. Narayanaswamy, L. Miller and A. Spanias, "Signal Analysis-Synthesis Using the Quantum Fourier Transform," ICASSP 2023 - 2023 IEEE International Conference on Acoustics, Speech 8 and Signal Processing (ICASSP), Rhodes Island, Greece, 2023, pp. 1-5.
- [35] "QED-C introduces a novel approach to measuring performance of Quantum Computers," HPCwire, <https://www.hpcwire.com/off-the-wire/qed-c-introduces-a-novel-approach-to-measuring-performance-of-quantum-computers/> [Accessed: 28-Sept-2023].

BIOGRAPHY



Leslie Miller received a B.S. in Electrical Engineering from Barrett, The Honors College at Arizona State University in May 2023. She is currently a research assistant associated with the SenSIP center. She is pursuing her master's degree in electrical engineering with a concentration in Signal Processing. She was awarded the Fulton Schools

of Engineering Impact Award in May 2023. She served as the President of the Epsilon Beta Chapter of IEEE-HKN from Fall 2022 to Spring 2023. Upon completion of her MS degree, she will work full



Glen Uehara is a Senior Distinguished Member of Technical Staff and Associate Director of the Quantum Engineering Center at General Dynamics Mission Systems (GDMS) with over 25 years of experience in Digital Communication and Signal Processing. Currently, he is

working in both Space Intelligence System and Quantum Research Laboratory at GDMS, researching how to apply classical and quantum algorithms to next-generation systems. Glen is a Ph.D. student and Senior Research Associate at SenSIP (Sensor Signal and Information Processing) Center at Arizona State University. He earned a master's in electrical engineering degree at Arizona State University and a bachelor's degree at the University of Hawaii at Manoa. He currently holds 3 patents in Signal Processing. He authored and co-authored over 5 publications related to Quantum Algorithms.



Andreas Spanias is Professor in the School of Electrical, Computer, and Energy Engineering at Arizona State University (ASU). He is also the director of the Sensor Signal and Information Processing (SenSIP) center and the founder of the SenSIP industry consortium (also an NSF I/UCRC site). His research

interests are in the areas of adaptive signal processing, speech processing, quantum machine learning and sensor systems. He is author of two textbooks: *Audio Processing and Coding* by Wiley and *DSP; An Interactive Approach* (2nd Ed.). He contributed to more than 350 papers, 11 monographs, 24 full patents, several provisional patents. He served as Associate Editor of the *IEEE Transactions on Signal Processing* and as General Co-chair of *IEEE ICASSP-99*. He also served as the *IEEE Signal Processing Vice-President for Conferences*. Andreas Spanias is co-recipient of the 2002 *IEEE Donald G. Fink paper prize*

award and was elected Fellow of the IEEE in 2003. He served as Distinguished Lecturer for the IEEE Signal processing society in 2004. He received the 2018 IEEE Region 6 Outstanding Educator Award (across 12 states) with citation: "For outstanding research and education contributions in signal processing." He was elected recently to Senior Member of the National Academy of Inventors (NAI).